Mobile on-Demand (MOD) mRNA Vaccine Production: A Design and Optimal Location Study

Steffen Fahr, B.Sc.[a]; Lukas Thiel, B.Sc.[a]; Carl Sengoba, B.Sc.[a]

[a] *Aachener Verfahrenstechnik, RWTH Aachen University, 52074 Aachen, Germany*

April 2021

Abstract

Vaccines are typically produced in large facilities to take advantage of economies of scale. However disease outbreaks are often local in nature and require flexible, small-scale production, especially in regions with poor infrastructure. In this work, mobile on-demand vaccine production is explored as a solution to future outbreaks. An mRNA vaccine process is scaled down to the size of two 20-foot shipping containers, so that 10,000 vaccine doses can be produced in one batch in less than 16 hours. The container is self-sufficient except for the regular resupply of water and electricity being able to produce 100 batches without resupply raw materials and consumables. The final cost per dose is estimated to be 25 € with a likely range between 4 to 45 € depending on dose size, raw material prices, and other underlying assumptions. The practicality of a container-based facility at the presented scale is demonstrated by two case studies.

1. Introduction

Overcoming a pandemic is a global task and putting a quick end to it is of paramount international importance. We are currently witnessing a missed opportunity among the wealthy nations to help the developing world to respond to the COVID-19 pandemic. Although organizations such as the World Health Organisation (WHO) appeal for international cooperation from the beginning of the pandemic, the current global distribution of vaccines does not reflect this. WHO health officials recently pointed out the potentially disastrous consequences of this so-called vaccine nationalism [1]: We are playing a game of chance against evolution, and we keep giving evolution extra dice. While the wealthiest nations, home to 16% of the world population, reach herd immunity, the spread of the disease continues in developing countries. As was confirmed in late 2020, the rising numbers of infections facilitate the emergence of new virus variants [2], against some of which the vaccines currently available are less effective [3]. Some mutations might even increase the virus's mutation rate itself [4]. If a variant emerges, which resists antibodies formed against the currently existing strains, the wealthy nations' neglect of the developing world could effectively cost them their precious herd immunity.

Providing vaccines to developing countries is not only a political, but above all, a technical and logistical challenge. Some vaccines require transport and storage at -80 $°C$ [5]. With a mobile, decentralized vaccine production unit, we provide an answer to the logistical challenges and give developing nations the opportunity to produce their vaccines on a national scale. Small-scale production of pharmaceuticals has received some attention in the past, e.g. [6]. These processes can be tailored in size for clinical trials [7], adapted to flexibly produce at different scales [6], or intended for large-scale production through scale-out [8]. In particular, the idea of small-scale vaccine production has evoked, for example, a patent on a small-scale transcription reactor for nucleic acid vaccine production [9], but an overall complementary concept for practical implementation is still missing.

In this work, a suitable process for vaccine production is identified and adapted for modular on-demand manufacturing. The inherent modularity and autonomy of the shipping container-based solution promises a flexible application across all levels of development and population density. Moreover, bypassing the step of scaling up the production process by instead numbering-up in containers, allows to potentially achieve a faster time to market e.g. due to long construction times of centralized plants [10].

The following chapters are structured as follows: First, different production platforms are evaluated with regard to their suitability for MOD manufacturing. A platform is chosen and a generic production process is identified. Next, a process flowsheet is developed to determine mass and energy balances. The production process and necessary utilities are then scaled and adapted for the container to work as independently of its environment as possible. Subsequently, the presented concept is analysed with a focus on the economic aspects. Finally, two case studies are presented, showing the applicability of the system in different scenarios while proposing a way to systematically locate the containers using mathematical programming.

2. Technology Screening

Over decades of development, biotechnology has produced an immense variety of vaccines and vaccine production platforms. Attenuated and still active viruses to combat the mumps virus, deactivated viruses against hepatitis and a protein against tetanus are some examples [11, 12]. Another class of vaccines has emerged in the field of nucleic acid vaccines. Examples include DNA vaccines against influenza or

HIV and the recently approved mRNA COVID-19 vaccines from BionTech/Pfizer and Moderna [5, 11]. The large variety of vaccines are produced by a wide range of processes. Thus the choice of the vaccine production process is highly case-sensitive, which makes a general ranking of different production processes challenging.
For the selection of the production process in the container, the three production platforms yeast, Chinese Hamster Ovary (CHO), and the *in-vitro* transcription of messenger ribonucleic acid (mRNA) are considered. The three major indicators for the design of such a production process are the techno-economical as well as the biological aspects and the pandemic response.These indicators are evaluated inside a benefit analysis [13], where each criterion is further subdivided and weighted. Each sub-criterion is rated from 1 (poor) to 5 (very good) with the intermediate scores of 2 (less bad), 3 (neutral) and 4 (good). The sub-criteria as well as the argumentation for the selection can be found in the supplementary information (SI 1). The summary of the selection is expressed in the mean values of the three criteria and visualized in Figure 1.

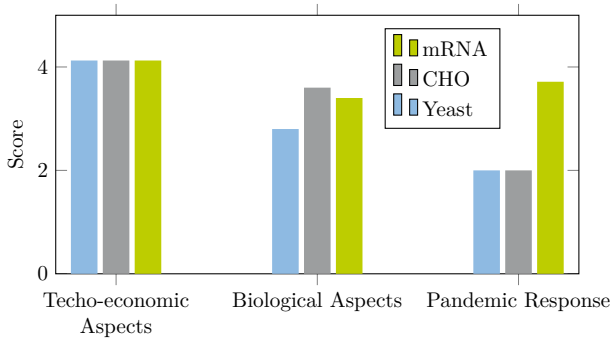

Figure 1: Results for the three production processes of the main indicators

All three processes differ fundamentally in the produced vaccine. Yeast, for example, is used to produce proteins that assemble into virus-like particles. Mammalian cells such as CHO are best suited for the production of inactive viruses. The mRNA technology is used to stimulate protein formation *in-vivo* [11, 14]. All three approaches are established on the market in terms of techno-economic applicability. There are differences in the ratings of the subcriteria for the evaluation of the techno-economic aspects, but when considering the mean value, a balanced result of 4.125 (good) is obtained for all processes, as shown in Figure 1.
Considering the biological aspects, yeast has a lower score than the other two processes. This can be explained by the CHO cells having a human-like folding and glycosylation pattern [15]. Proteins produced by yeast cells, on the other hand, must be humanized, which compromises productivity and secretion [16]. The release of the vaccine components into the culture medium requires a cell disruption for yeast, whereas the CHO cells and the *in-vitro* transcription of the mRNA do not. More specifically, no cells will be required for the production of the mRNA.
When it comes to the aspect of pandemic response, reports from both the outbreak of COVID-19 in 2019 and MERS-CoV in 2012 show clear trends of mRNA being the quickest to reach phase III trials, followed by inactivated virus vaccines, which are usually produced by mammalian cells. Protein vaccines, produced by yeast cells are ranked last due to the in-depth knowledge about the virus that is required for their development [17–20]. The *in-vitro* mRNA process is expected to exhibit even faster development times for new pathogens after this pandemic, as a previously designed process can be used for a new vaccine with close to zero changes to the process itself. This concludes the results of the third and last category, the pandemic response, with mRNA achieving a rating of good and the other two a rating of less bad.
In summary, mRNA emerges from this evaluation as the best conceivable approach. In the following, a process concept for the production of a mRNA vaccine will be developed.

3. Generic mRNA Production Process

In the following sections, a generic process for the production of mRNA vaccine is presented. A gene expression of the coronavirus spike protein, composed of about 2000 nucleotides (nt), is used as an example in this study. However, the process can be used to construct and purify any mRNA vaccine. The process can be divided into the transcription reaction, the purification of the mRNA transcripts, the formulation of the mRNA into lipid nanoparticles (LNP) and the packaging (see Figure 2). The first three steps will be covered in more detail in the following sections. The packaging step includes filling the product into vials and putting those into intermediate storage. As fully automated packaging under sterile conditions is state of the art and corresponding solutions are sold as turnkey systems [21], the packaging step will not be covered.

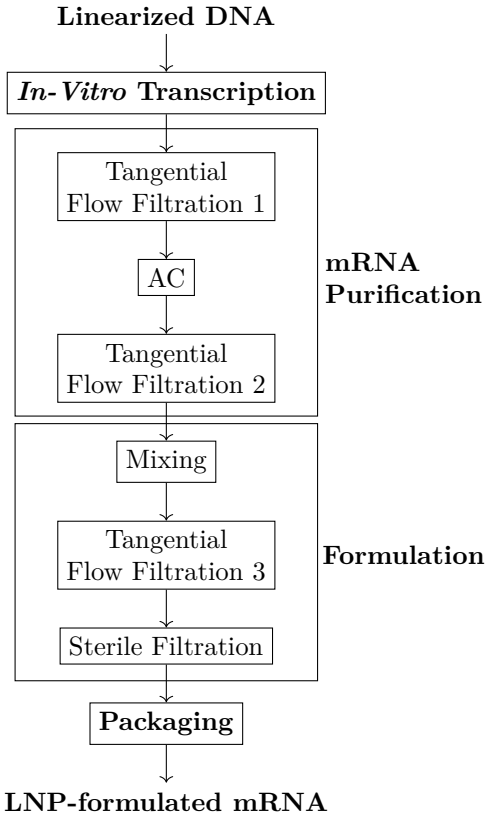

Figure 2: Block flow diagram

3.1. In-Vitro Transcription

The mRNA is produced as a result of the so-called *in-vitro* transcription (IVT) with co-transcriptional capping. *In-vitro* transcription (IVT) with co-transcriptional capping is the process step in which the mRNA is produced. The key element of the transcription is the linear DNA template. It contains the information necessary for later translation *in-vivo* to produce the desired protein. For good selectivity and yield of the transcription reaction, linearized double-stranded DNA is used as a template, which is commercially available [22, 23]. Usually, DNA amplification is carried out through fermentation or polymerase chain reaction (PCR) [11, 24, 25]. However, this degree of vertical integration is infeasible in a shipping container, considering that fermentation-based DNA must be purified extensively [26]. Moreover, the amount of DNA needed can easily be stored onsite, making onsite amplification unnecessary.

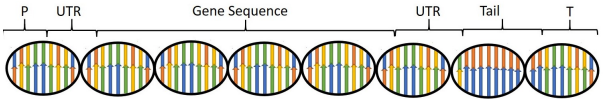

Figure 3: Illustration of a DNA template [27, 28]

An illustration of the DNA template can be found in Figure 3, which is divided into different sequences and starts on the left side with a promoter (P) followed by an untranslated region (UTR). Continuing on the right, the gene of interest is visualized. This region will later code the protein of interest in the human cells. Then, an UTR and a poly (A) tail are shown. The terminator (T) finishes the DNA template [24, 28–30]. Besides the importance of the DNA template, other raw materials are inevitable for the production of the mRNA. These raw materials include nucleotide triphosphates, CleanCap® (Cap1), polymerase, which are all mixed together and diluted in a buffer solution.

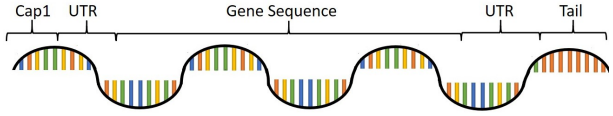

Figure 4: Illustration of a mRNA [31]

Polymerase is the enzyme that generates the mRNA depicted in Figure 4. T7 polymerase is commonly used for this task [24]. It binds to the promoter (P) of the DNA template and initiates the elongation. mRNA is formed through elongation and on the opposite end to the tail a cap molecule is attached. For the so-called co-transcriptional capping the commercial reagent CleanCap® with a cap 1 structure can be used. Alternative co-transcriptional methods like anti-reverse cap analog (ARCA) only result in a cap 0 structure. The difference being that further methylation of the cap 0 results in a cap 1 structure [32, 33]. A possible enzymatic reaction could convert the cap 0 structure to a cap 1 structure, although this would lead to an extension of the process, which can be avoided with CleanCap® [24, 32]. Additional advantages of CleanCap® are higher efficiency and a larger yield of capped mRNA in comparison to other products. The polymerase detaches at the terminator with the completed mRNA [24, 30, 32]. The regions UTRs, tail and the cap structure are of high importance for the mRNA, as they increase the translational efficiency and the stability of the mRNA in the cells. As a result, a higher yield of proteins can be reached *in-vivo* [30, 34, 35]. In the next step, the produced mRNA is transferred to the downstream process.

3.2. mRNA Purification

From the reactor, the mRNA is obtained diluted in the transcription buffer along with a range of additional components. The fully functional mRNA transcripts are expected to be present at a concentration of approximately 5 g/L. Impurities include the enzymes used in the reactions along with the buffer components added to the reaction and residual nucleoside triphosphates (NTP). Additional protein impurities may be present in commercially available enzyme preparations [36]. Moreover, two major impurities occur during the reaction, namely short abortive RNA transcripts [36–38] and double-stranded (ds)RNA [39]. Abortive transcripts have a length of approximately 8 nt for T7 RNA polymerase [40] and are therefore smaller than the desired mRNA by orders of magnitude. dsRNA presents a more challenging impurity to remove, as its molecular weight is similar to the weight of the full-length single-stranded mRNA. The impurity occurs, as in rare events, the polymerase can produce strands of RNA that are complementary to the target RNA by annealing to the DNA template without the presence of a promoter. The complementary RNA will anneal to some product molecules, creating dsRNA [41]. While these rare events are not noticeable in the overall mass balances, it is critical to remove traces of dsRNA as it triggers an innate immune response in the human body [39, 41] which deteriorates the efficacy of the vaccine.

The downstream processing of mRNA comprises a tangential flow filtration (TFF), a chromatography and a subsequent second tangential flow filtration (see Fig. 2). The first TFF is in principle adapted from [42]. Therein, the TFF device performs purification, concentration and buffer change in a single 1-hour step for a fluid volume on the order of what will be encountered in small-scale production. The authors use a modified polyethersulfone membrane and recommend a molecular weight cut off (MWCO) of no more than 2/3 the molecular weight of the product. For an mRNA sequence of a length of 2000 nt (molecular weight of approximately 640 kDa), the most suitable commonly available MWCO is 300 kDa. Therefore, some protein impurities such as the RNA polymerase (100 kDa) will be at least partly removed in this step. The transmembrane pressure reported in the patent [42] is 14 kPa, which can easily be generated by a peristaltic pump.

The retentate of the TFF is further purified in a chromatography column. For a conservative case, an affinity chromatography (AC) column is used for this task. Affinity resins comprising immobilized Oligo-dT structures, which selectively bind to the Poly-A tail of the mRNA, are commercially available [43]. Comprehensive instructions on the operation conditions of such a column are given by the resin manufacturer. After packing and equilibrating the column, loading takes place at a high salt concentration and a linear velocity of 50-150 cm/h. Impurities are washed from the column using a decreased salt concentration and finally, the product is eluted at a low salt concentration. A yield of 92% for an oligo-dT AC is given in [44].

As a cheaper alternative to the AC, an Anion Exchange Chromatography (AEC) can be employed [25]. AEC resins are generally cheaper than AC resins and the procedure is of similar complexity [38]. The separation mechanism is based on the negatively charged backbone of RNA attaching to positively charged groups that are immobilized on the resin. Several works have employed AEC successfully for the purification of RNA [38, 42, 45]. Moreover, this method appears to selectively separate the product from dsRNA. A comprehensive instruction on how AEC can be operated to achieve this is given in [45]. While for the conservative case, the AC is assumed, the cost savings of potentially being able to use AEC will be discussed. Notably, the yield of an AEC reported in the literature ranges from 72 to 90% [38, 42, 45], with the lower end potentially leading to cost increase and the higher end to cost savings over the AC case.
Finally, a second TFF is employed, which conceptually does not differ from the first one. It is assumed that after the AC, all aforementioned impurities are removed from the product solution. Therefore, the second TFF has the sole purpose of changing the buffer according to the following processing step's requirements.

3.3. Formulation

Due to the low stability of the mRNA molecule and the ubiquity of RNAse, protecting the mRNA via encapsulation is indispensable for achieving the vaccine's full potential. The effect of the increased stability through encapsulation is twofold. Firstly, the encapsulation leads to an increased shell life due to better thermostability. Secondly, early degradation in the human body is suppressed, greatly enhancing the uptake of the mRNA vaccine by the body's cells [16, 46–48]. Lipid nanoparticles (LNPs), as visualized in Figure 5, are the most advanced mRNA vehicles at the moment. In the figure, ionized lipid molecules are color-coded in orange, whereas the mRNA is depicted as curly red lines.

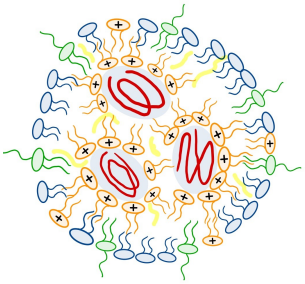

Figure 5: Illustration of a lipid nanoparticle [47]; red - mRNA; orange - ionized lipids; blue, green and yellow - helper lipids

The mRNA forms a complex with ionized lipid molecules, interacting with their positively charged end. In the resulting complex, the hydrophobic ends of the lipids point outwards. To these ends, the helper lipids shown in blue, green and yellow attach with their hydrophobic ends, forming a stable liposome [47]. The composition of the lipids is chosen based on the published research articles and recommendation from Precision Nanosystem [49, 50]. The share of lipids is close to the ratio of lipids in the approved Moderna Covid vaccine. The molar ratio of the lipids is 50:10:38.5:15 (ionizable lipid:DSPC:cholesterol:PEG2000) [27, 28, 50–52].

There are different ways to carry out the formulation process. Reichmuth et. al [53] have shown a possibility to form LNPs through a fluid mixing step. First, a cleaned mRNA buffer solution and a solution of ethanol, in which the lipids are diluted, are prepared. Then, throughout mixing, the mRNA and lipids will form the desired nanoparticles [50, 52, 53]. Afterwards, the ethanol will be removed by means of another TFF. The final step for the encapsulated mRNA vaccine is the sterile filtration which is a regulatory step. The filter has a pore size of about 0.2 μm [54] where the vaccine is obtained in the permeate and impurities like microorganism are caught in the filter and discarded with it [28, 51, 54, 55]. A schematic of the formulations steps is given in Figure 2. Subsequently the quality control is indispensable and is described in the following.

3.4. Quality Control

According to current regulatory agencies, different quality control steps must be employed throughout the process in order to ensure product purity and integrity [56, 57]. To this date, no specific regulations have been given with regard to RNA vaccines produced through IVT by the Food and Drug Administration (FDA) and European Medicines Agency (EMA) [58]. Therefore, quality control steps are customized for the present process with the possible impurities mentioned in section 3.2 in mind. The effluent of the second tangential flow filtration containing the purified naked RNA will be subject to a series of quality control steps, ensuring the absence of any unwanted compound. The absence of DNA can be proven through the use of a fluorescent dye [58]. Furthermore, UV absorbance is employed to quantify the total nucleic acid content which, in the absence of DNA, equals the RNA content. In case enzymes are still present in the solution, the UV absorbance will show additional characteristic absorbance maxima [58]. Finally, the absence of dsRNA can be proven by using dot blot [39]. As mentioned in section 3.2, dsRNA generates an immune response. The associated antibodies are commercially available as primary antibodies for blotting. The listed quality control steps, particularly the waiting time associated with blotting can take place in parallel to the process (see section 4.2).
For quality control of the final product, the particle size of the LNP is measured via dynamic light scattering [59]. Finally, some of the final product is analyzed in a gel electrophoresis [60] after disrupting the LNP by resolution in Triton-X buffer to verify the integrity of the RNA and the absence of major impurities originating from formulation or packaging. If required by local regulatory agencies, high performance liquid chromatography (HPLC) can be used in place of the gel electrophoresis.

4. Design of the Container-Based Process

A process based on the sequence presented in section 3 is designed to take place in a 20 ft ISO shipping container with an additional container for auxiliary tasks. Throughout designing the process, special attention is paid to the severe spacial restriction and sterility requirements, in particular with regard to RNAse contamination. The process is designed to produce 10,000 doses of 100 μg mRNA each

per batch. This corresponds to the mRNA content used in Moderna's vaccine [5], while BioNTech-Pfizer and CureVac use doses containing 30 and 12 μg RNA, respectively. The choice of plant capacity was an integrated decision taking into account storage and logistics and is discussed in a later section.

4.1. Design and Sizing of Process Equipment

For sterility reasons, process steps are carried out using single-use equipment wherever possible. All buffers are premixed in the utility container using RNase-free water produced onsite to make best possible use of the available storage volume and increase the autonomy of the container. No more than one employee at a time works in a container. For sizing, mass and energy balances, and scheduling, a process model is set up in SuperPro Designer [61] (see SI 2).

The IVT and capping are performed in 0.3 L of aqueous solution in a disposable stirred-tank bioreactor such as a Merck Mobius® [62]. The reaction volume and the corresponding input materials are taken from the description of the company TriLink Biotechnologies. Buffer compositions, proportions of nucleotides, DNA template and CleanCap®, as described in the literature [24], are scaled for the quantity of 10,000 vaccine doses.

As an alternative to a disposable reactor, CureVac has filed a patent concerned specifically with IVT-based mRNA production at a small-scale [9]. The device called RNA Printer® is an IVT reactor with DNA template immobilized on magnetic beads for reuse. However, without a shortage of DNA template supply, DNA recovery is not necessary for a feasible concept and not of high priority when it comes to cost savings (see section 5.2, SI 3).

After the transcription and capping reaction, the reactor content is filled into a disposable bag for downstream processing. We envision the three TFFs and the AC to take place at a section of the container wall with a single or two peristaltic pumps mounted in a fixed position and mounts in place for various disposable items (filter cartridges, bags etc.). Moreover, a steel tank is in place as a reservoir for the TFF, which is lined with a new disposable inlay bag each time it is used. For simple handling and to support the operator, the back wall may contain drawings indicating the tube routing along with LED lights instructing the operator where to mount and connect equipment for each process step. Note that during use, only one unit operation is in place at a time. Above and below the mounts for process equipment, disposable bags with buffers and the product solution can be mounted on hooks with weight sensors. After mounting bags and tubes, the process can operate autonomously with flow being controlled by the peristaltic pump and feed streams being chosen through electronic valves. A schematic drawing of the fluid processing is given in Figure 6.

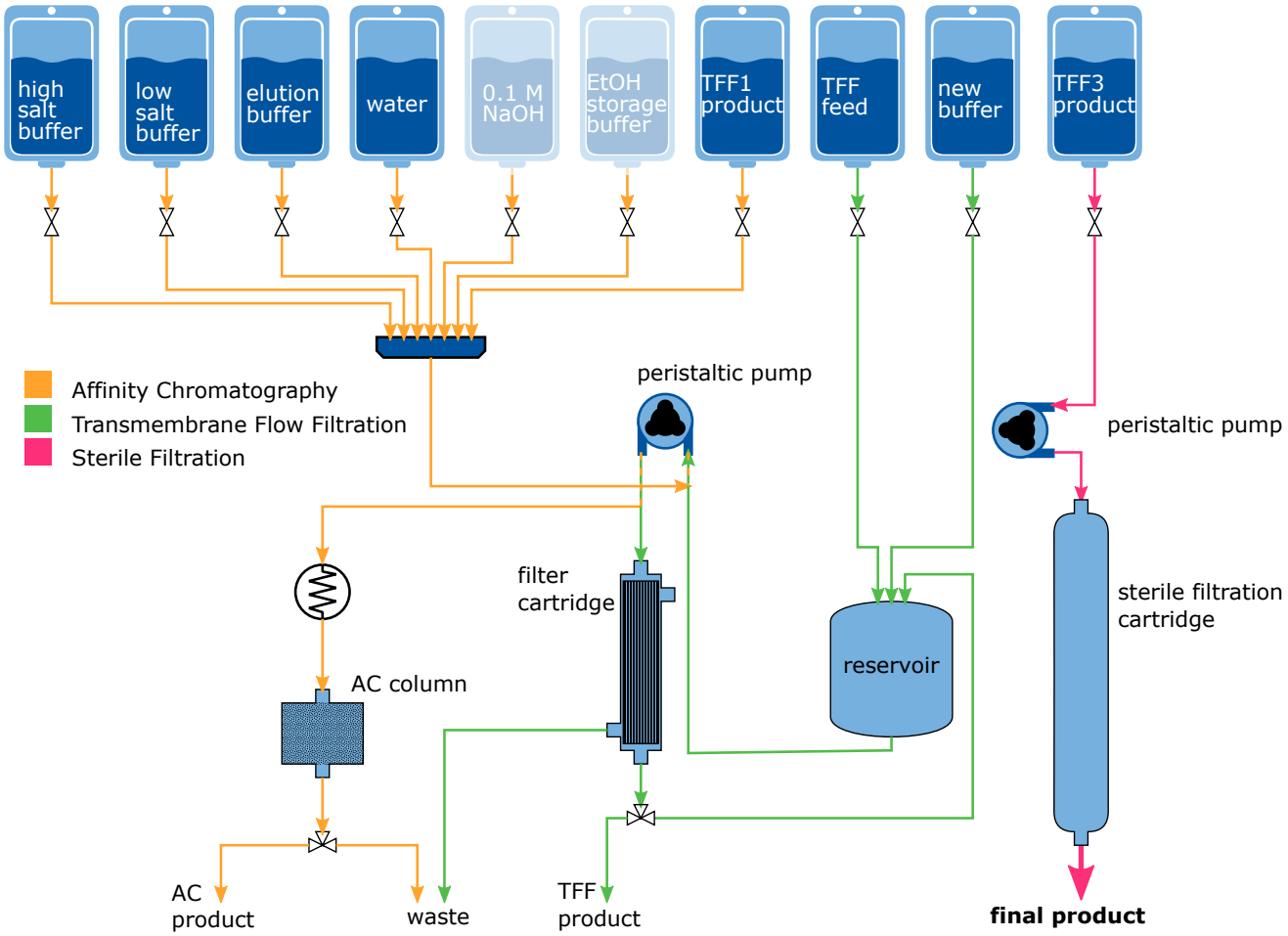

Figure 6: Schematic drawing of the modular wall-mounted fluid processing system. Only one of the individual colored operations is mounted at a time.

For sizing, the results from the SuperPro Designer model are used after comparing them with literature values. The TFFs process a feed volume of 0.3, 2.7 and 2.2 L per batch for TFF 1, 2 and 3, respectively. The filter area is calculated by SuperPro Designer according to the chosen process times of $60 - 100$ minutes to be $590 - 2090$ cm^2. For reference, in [42], an experiment is presented, wherein an area of 790 cm^2 is used to process 400 mL of liquid in 58 minutes. For the ratio of fresh buffer fed into the system to original buffer of the concentrated solution, a value of 8 is proposed in [42]. Moreover, a recommended shear rate of 800 s^{-1} is given, which can be used to estimate the volumetric flow generated by the peristaltic pump for the filter cartridges assumed herein. A flow rate of 200 mL/min is used in the experiment performed in [42]. For the product recovery of TFF 1, a value of 93.4% is assumed, which lies in the range (90-95%) given in [42]. The other two TFFs are designed with the same equipment parameters as TFF 1. This naturally results in higher overall yield as compared to TFF 1, as TFF 2 and 3 are used for buffer change, which is a less demanding task than purification, requiring less passes of the liquid along the filter.
The AC is sized according to the resin's specific binding capacity of 2 mg/mL given by the manufacturer of the POROS™ Oligo (dT) resin [43]. For comparison, Moderna reports a binding capacity of 1.4 mg/mL for their own Oligo (dT) resin [44]. The authors of patent [44] present an experiment with a column of 100 mL volume and 5 cm length. The length is adapted for the present process, although in practice, the final length-to-width ratio can be subject to further adjustments. The fluid velocities and buffer composition in the patent closely agree with the recommendations given by the manufacturer of the POROS™ resin, which are adapted for this work. The operation time of the column results from choosing these parameters. The yield of the AC is assumed to be set to 92%, based on an experimental value reported in [44].
Reusing the resin is possible according to the manufacturer and instructions on storage and cleaning steps are given. However, for a base-case process, single-use of prefilled columns is considered. If the resin is reused, two additional buffer solutions are needed for sanitizing and storage, which are depicted in a more pale blue in Figure 6.
For example, with their KrosFlow® KR2i [63], the company Repligen sells a benchtop TFF system, which can generate enough pressure and flow rate for the AC and all the TFFs used in our process. For the sterile filtration, an additional, more powerful peristaltic pump would be needed, although in principle, all operations could be carried out using a single peristaltic pump inserting a new length of tube for each step.
The formulation as LNP takes place in between the filtration steps TFF 2 and TFF 3 (Figure 2). Devices such as the NanoAssemblr® GMP system are commercially available as a turnkey system [64]. Operating such a device includes inserting a new microfluidic cartridge and tubing and mounting the RNA-containing and the lipid-containing solution in place. The costs of owning and operating the device have been obtained through personal communication with the manufacturer.

4.2. Scheduling

The production process consists of individual unit operations performed sequentially as batch operations. A realistic schedule of the overall process is proposed in Figure 7, which is based on the SuperPro Designer Simulation. Additionally, an indication is given of the time periods in which the operator working in the production container needs to take action operating or setting up one of the unit operations. This time includes ten minutes for each "transfer" operation in SuperPro Designer, i.e., transferring the main process stream from one unit operation to the next. Setting up a new unit operation for fluid processing is estimated to take 30 minutes, which can be parallelized whenever the previous unit operation does not use any fluid processing

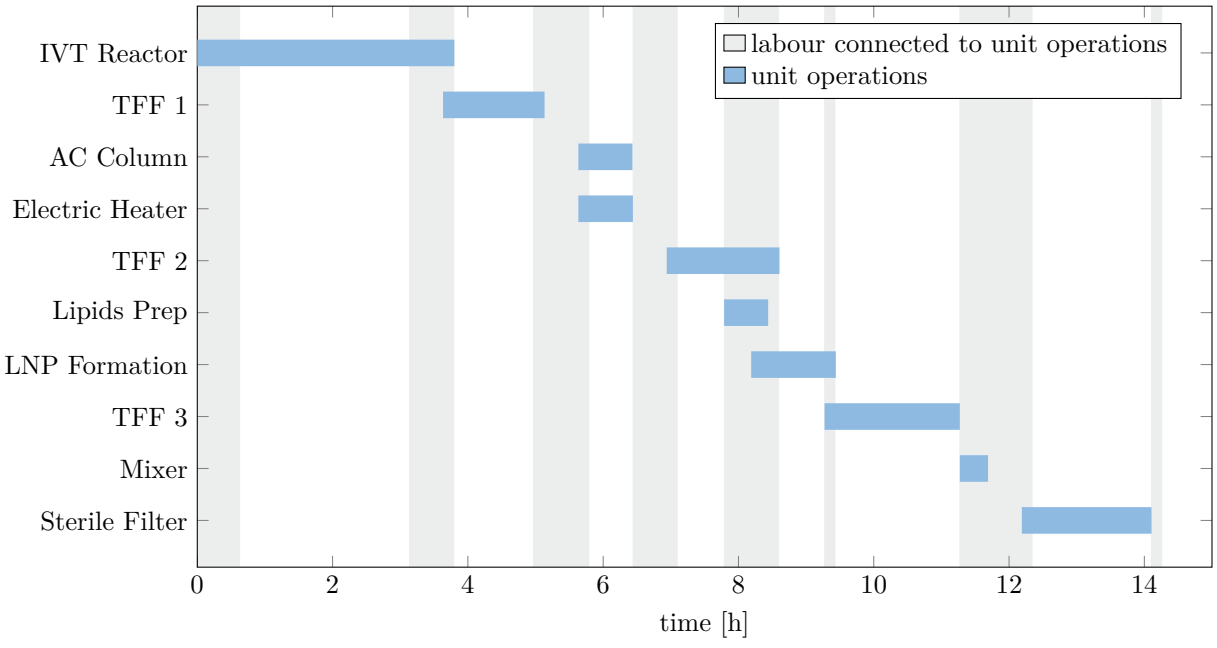

Figure 7: Scheduling of unit operations and labour requirement in the production container.

equipment. Premixing of buffers is not included in this schedule. It can be performed at any time by the operator working in the utility container, since space for intermediate buffer storage is provided. Besides buffer mixing, this second operator is responsible for packaging, storage and handing out packages of vaccine for delivery.
As can be seen in Figure 7, the production process not including filling takes approximately 14 h. Adding the time requirement for filling and packaging, finishing a batch within 16 hours or two 8-hour shifts is realistic. At all times, one operator works in each container, totalling 32 work hours per batch. As shown in Figure 7, the operator of the production container is free to perform auxiliary tasks such as waste management and quality control during approximately half of the time, while the unit operations work remotely. The active work at them is centered around the change from one unit to the next. The fact that the fluid processing system is shared by all filtrations and the AC column leads to time gaps during which the operator changes the equipment and no unit operation can run (see Figure 7, at 5.1, 6.4 and 11.7 h). Eliminating these three gaps of 30 minutes each would come at the cost of additional space requirement for downstream processing and with the process fitting nicely into a two-shift time span, there is no significant motivation to do so.

4.3. Container Layout

With the present concept designed for mobility and autonomy, it remains to show that the equipment described in the previous sections fits into the two containers, along with sufficient raw materials and consumables to sustain production without any resupply for an extended period of time. As further discussed in section 6.2, the target without resupply are 100 batches of 10,000 doses each (i.e. 1,000 10-dose-vials).
An exemplary layout for both containers is presented in Figure 8. The container depicted at the top, called "production container" in the following, contains the reactor, downstream processing and formulation units arranged in the order of use. Moreover, raw materials and single-use equipment needed in the process are stored in the container, with an additional cold storage unit for intermediate storage of buffers. Finally, the container contains quality control equipment.
The second container, called "utility container" in the following, comprises room for premixing of buffers, using RNase-free water, which is produced by the filtration units

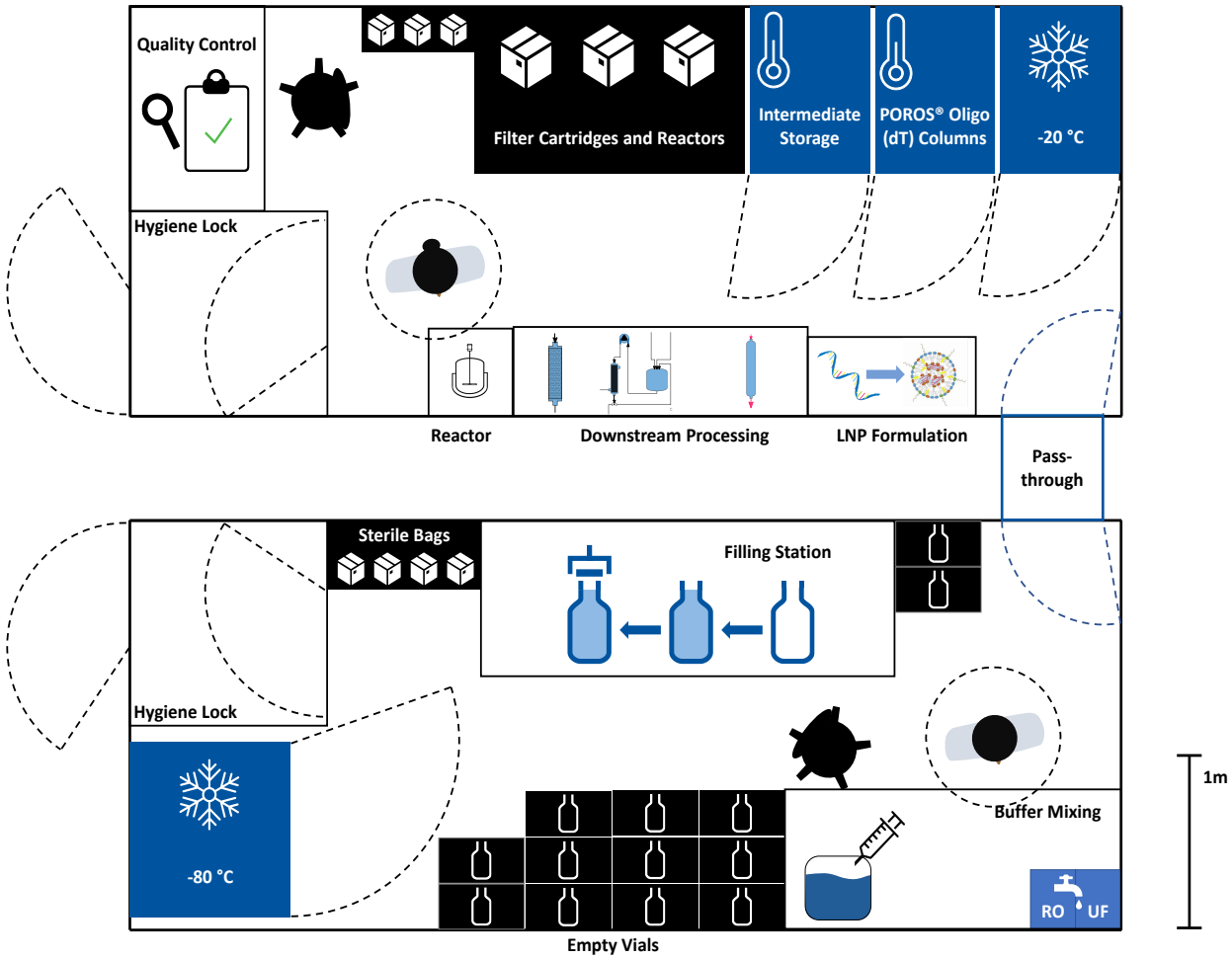

Figure 8: Schematic layout of the production (top) and utility (bottom) container. Container dimensions shown are the inner dimensions of 235x590 cm

included in the same container. Furthermore, the storage of empty vials, filling of vials and temporary storage of the final product take place in this container. The containers are connected by a pass-through, which is installed while the containers are set up at the production site. Disposable bags with buffer are passed from the utility to the production container and later, a bag containing the final product for filling and packaging is passed back to the utility container. The filling of vials can take place in a fully automated GMP-certified device, which is commercially available [21]. The storage space needed for single-use equipment and vials is estimated based on simple assumptions concerning the packing efficiency (see SI 5). Note that a particularly large space is occupied by the vials. As vials are used, the available space in the container increases. Freed-up space can be used to store waste in the container. Similarly, resupply of empty sterile vials would be an effective way to free up more space, if needed for other purposes.
While the layout as shown represents just one of several possible configurations, it helps to visualize two important points: Firstly, the space offered by two containers is large enough for the IVT-based production of mRNA vaccine. Secondly, for the presented fully autonomous concept, storage space limits amount of vaccine produced without resupply to one million doses, corresponding to 100,000 vials or 100 g of mRNA.

4.4. Utilities

For the container to unfold its full potential in terms of its mobility and flexibility, its requirements for utilities from the outside must be reduced to a minimum. Therefore, onsite production of RNase-free water is included in the concept and a HEPA-filtered heating, ventilation and air conditioning (HVAC) system. Moreover, to maintain a sterile environment as well as cooling of raw materials and temporarily stored product, continuous and reliable supply of electricity is crucial. Water, air, cooling, and electricity are briefly discussed in this order in the following.
RNase-free water is crucial for each of the production steps discussed in section 3, as well as additional cleaning steps. As such, it is by far the most needed raw material by volume with a demand of 46 L/batch for the process steps alone. Not only is a reliable third-party supply logistically challenging in developing nations, but intermediate storage of water can also easily lead to contamination with RNase [65]. In the literature, there exist two major approaches for producing RNase-free water. Firstly, water can be treated with diethyl pyrocarbonate (DEPC), which deactivates RNase and secondly, a well-maintained filtration device can be used to purify water [65, 66]. In both cases, tap water is assumed as raw material [65]. The DEPC method not only requires an additive, but residual DEPC must also be broken up into ethanol and CO_2 in an additional thermal step. Finally, the deactivated RNase and DEPC degradation products might need to be removed in additional steps. Meanwhile, the filtration-based method can be conducted in an automated manner with two consecutive filter devices. For our case, the filtration was chosen over the DEPC method for its simplicity. In particular, two consecutive Merck RiOs 16 system can be used, which can produce up to 16 L/h or 320 L/day. The first one operates in its standard reverse osmosis configuration, while the second one is equipped with a 5,000 Da ultrafiltration cartridge [65].
To provide an RNase and germ-free production environment, both containers must be equipped with cleanroom technology. For this purpose, a hygiene lock is installed at each entrance. Moreover, HEPA-filtered HVAC systems are installed on the roof. These can be transported in the inside of the containers during transport on a container ship, where containers may be stacked. The system has the twofold task of maintaining an adequate temperature and air quality. Therefore it must have sufficient tonnage, i.e., ability to remove heat from the container and sufficient air turnover. The heat to be removed can be estimated based on heat transport through the container wall plus electric energy dissipated inside of the container. Note that, while designed for hot environments, the system will also suffice in cold environments, as we found that a hot rather than a cold environment represents the limiting case for the system. The heat dissipated by refrigerators and other devices in the containers both significantly lowers heating demand in cold environments and increases the cooling necessary in hot environments. The heat transport through the container wall can be estimated based on a standard transport coefficient for shipping containers of 0.4 W/m^2K [67, 68], which is roughly equivalent to a 5 cm layer of polyurethane. The average temperature difference across the container wall is assumed to be 15 K. The additional heat generated inside the container by equipment and staff can be estimated based on the equipment's electricity demand and a rule of sum, respectively (see SI 4). Overall, a tonnage of 0.46 tons is required for the more demanding of the two containers.
According to the WHO [69] 6 - 20 air changes per hour are required in GMP facilities, i.e., 6 - 20 container volumes per hour or 180 - 610 m^3/h . A system consisting of a 2-ton HVAC unit [70] combined with a suitable supplemental fan and HEPA filter (see SI 4) is used for each container, satisfying both air change and air conditioning requirements. The final energy consumption of the HEPA-filtered HVAC itself is calculated using the cumulative heat load and a constant coefficient of performance of 3.5, as has been shown for a temperature difference of 15 K [71].
Cold storage at different temperature levels is required. While most raw materials require storage at -20 $°C$, the consumable affinity resin requires storage at 2 - 8 $°C$ [43]. The final product might require storage at -80 $°C$ in a conservative or worst-case scenario, although the Moderna COVID-19 vaccine has been shown to be stable at 2 - 8 $°C$ for 30 days [5], which is long enough for the present concept in which batches are produced few days apart. For a million doses of vaccine, 15 kg or approximately 15 L of raw materials are used that need to be stored at -20 $°C$, among which are 5.6 kg nucleotide, 4.6 kg polymerase, 1.2 kg CleanCap® and 0.8 kg DNA template solution. A 650 L freezer is therefore sufficient to store raw material for one million doses (see SI 5). Affinity resin is assumed to be stored in prepacked columns. We assume that one column of 5 cm inner length [44] and 13.5 cm diameter (SuperPro calculations) is used per batch, which is packed in a 15x15x15 cm package. A 650 L refrigerator can be used with spare room to store the raw materials stored at that temperature (see SI 5). If

a high-performance freezer of outer dimensions of 198.1 x 100.6 x 95.5 cm (H x W x D) is used for product storage, up to 21 batches or 210,000 doses can be stored at a time, which corresponds to about a fifth of the vaccine produced during a campaign. More details on the storage volume calculations for raw materials, consumables and product can be found in the SI 5.
Maintaining a reliable supply of electricity is especially challenging during road transport and in the presence of a non-reliable local electricity grid. Therefore, each container is equipped with a battery storage system. Tesla Powerwall [72] technology is chosen for this project. One layer of 14 Tesla battery packs underneath the inner container floor provides a total battery capacity of 189 kWh with a cumulative peak power of 64 kW per container. The downtime electric load caused by refrigeration and air conditioning is 18 kWh/day for the utility container and 32 kWh/day for the production container. Accordingly, the production and utility container last for 5.9 and 10.5 days during downtime, respectively. When operating the container, an additional load per batch is caused by the process equipment, which reduces off-grid days to 4.9 and 6.9 days for the two containers (see SI 4). These numbers indicate that several days of road transport are possible for the containers, although for very long journeys, a charging stop must be scheduled every few days. During transport on a container ship, the containers need electricity supply for at least the raw material cooling. If electricity supply is lost during or before a planned batch, the batch can be finished as scheduled using electricity from the batteries.

5. Process Analysis

In the following three sections, a detailed analysis of the process and its economics is presented.

5.1. Mass and Energy Balances

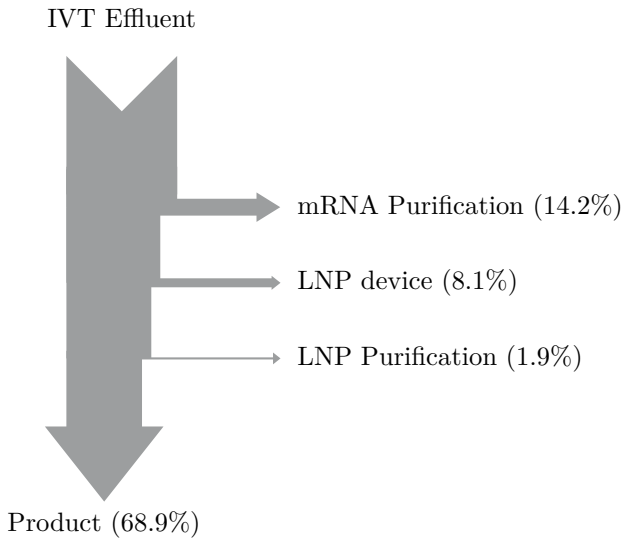

Figure 9: mRNA loss in downstream process

A graphical overview of the mass an energy balances is given in order to visualize potential areas of improvement and bottlenecks limiting the production scale of the containers. As can be seen in Figure 9, the individual downstream sections all exhibit a high yield with low potential for further improvement. Losses result mainly from the first TFF, the chromatography, and RNA that is not incorporated in LNP. The remaining filtration devices are designed for buffer change rather than removal of impurities and exhibit a low loss of product. The percentages given in the figures relate to the initial amount of RNA produced.
As visualized in Figure 10, the majority of electricity consumption is necessary for cooling and air conditioning and therefore independent of the actual production. Accordingly, the energy consumed per batch produced increases as the time between finished batches increases.

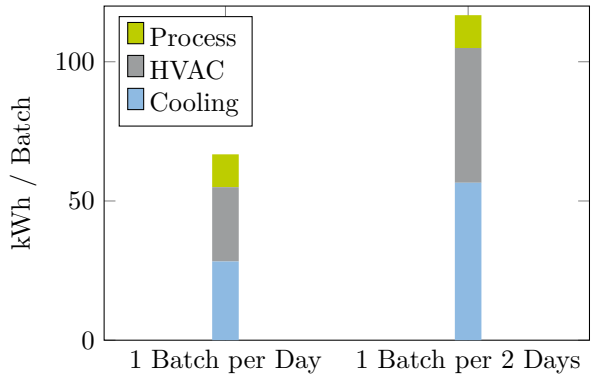

Figure 10: Electricity demand of one batch

Finally, comparing the liquid volumes of different buffers and process streams used gives insight into different scale-up limitations, which are further discussed in 6.1. Notably, the buffer volumes used in the downstream operation exceed by up to one order of magnitude the sample volume and are the limiting factor when it comes to scale-up. Interestingly, the final product (i.e. LNP-encapsuled mRNA at the correct concentration for injection) is much more dilute than the mRNA leaving the IVT reactor, which helps explain the limiting nature of the filling unit for large-scale production [25]. A graphical representation of the mentioned volumes in a sankey-type diagram is given in SI 6.

5.2. Economic Evaluation

In this section, the major cost contributors are identified and the cost per dose of vaccine is determined. The assessment of the costs is based on commercially available products which are suitable for the usage in the container. For realizing mobile on demand vaccine manufacture, the costs can be divided into investment costs for purchasing equipment and building the container and variable costs for producing the vaccine. The investment costs may further be subdivided into three larger groups as shown in Figure 11. The expenses to implement a cleanroom container, color coded in light blue, claim about 37 % of the costs. The base costs in this category consist of the interior equipment, the container itself, the water production and the HVAC system. As a GMP facility and cleanroom equipment have high requirements the base cost are adjusted by a factor of 250 %. This approach is also used for the cost approximation of the electronics (10 % of base cost) and for the missing cost items (30 % of base cost) [25]. The costs of equipment, colored in grey, accounts for 58 % of the investment costs. The fully automated filling system

and the GMP device for encapsulating the mRNA are major cost drivers in this category. Peripheral items necessary for cooling the raw material and for quality assurance contribute with 5 % to the investment costs are visualized in green. In total, the investment costs add up to 2.43 million euros.

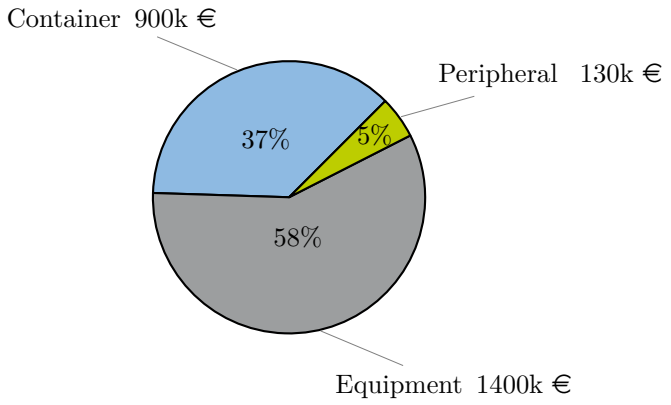

Figure 11: Investment Costs

The reference case for the development of the container is a production volume of 10,000 vaccine doses per batch. For this, the cost of single-use equipment and the raw materials was estimated via SuperPro Designer. Note that the variable cost vary to a different degree with batch size and number of batches produced. For example, the affinity resin required scales in a linear fashion with the batch size, while the cost of producing a batch of LNP remains the same over a large range of batch sizes. The variable costs can also be subdivided into three groups illustrated in Figure 12. The process costs such as consumables like filters, pump heats, etc account for 61 % (blue), raw materials for 38 % (grey) and the labour for 1 % (green) of the variable cost. These add up to a total of 228,700 € per batch. Therein, the microfluidic cartridge for the formulation device and AC resin can be identified as the major cost driver. A detailed overview of the costs can be found in the SI 7.

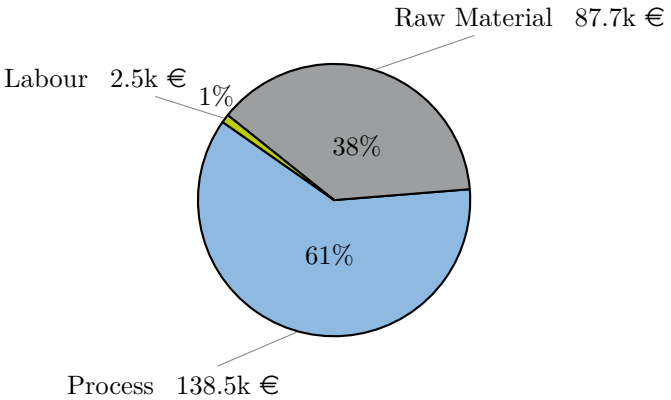

Figure 12: Variable costs per batch

Combining both categories, investment and variable costs, and assuming that the investment cost are spread over one million vaccine doses, the price per vaccine dose is 25.12 €. One way to compare the resulting price is to evaluate against current products on the market. So far, this is possible with BioNTech/Pfizer's vaccine. After negotiations with the European Union, a price of 15.5 € per dose has been agreed on, according to reports by Norddeutscher Rundfunk, Westdeutscher Rundfunk Koeln and Sueddeutsche Zeitung [73]. It should be highlighted that the BionTech/Pfizer's vaccine has a dosage of 30 μg compared to the 100 μg used in the container concept. Assuming that the vaccine produced in the container achieves similar efficacy, a price of 17 € would be possible.
Another possibility is to compare the cost structure of a modelled centralised production facility with that of the mobile container concept, which is depicted in Figure 13. For this comparison, the paper of Kis et al. is used, which shows the calculation and cost structure for the vaccine production of an mRNA vaccine for the world population [25]. The relative shares of investment and labour costs do not differ to any great extent for both concepts. However, in centralised production, raw materials are associated with a significantly larger and consumables with a significantly smaller share than with the mobile concept. This can be explained by the central production dividing the cost of single use equipment by a larger number of vaccine doses. The proposed price per 100 μg-dose by Kis et al. is on the order of 2 € which is significantly less than the price for the container concept despite highly similar process characteristics such as titres, yields and purity requirements [25]. This deviation can only partly be explained by economies of scale and is also a result of more optimistic assumptions concerning raw material prices which do not correspond to the prices that manufacturers can currently achieve. For example, the price used for CleanCap® is one tenth of the price assumed in our work [25]. The prices for the polymerase or lipids used in centralized calculation are also much lower than those researched for the present concept. The cost of raw materials alone was calculated to be 8.8 € per dose in this work. Accordingly, the aforementioned effect of dominating raw material costs at large scale is more pronounced with our assumptions than with Kis's [74]. Finally, the delivery of the vaccine in a central production scenario must be taken into account, which is already partly included in the container concept as the container is deployed near the vaccination site.

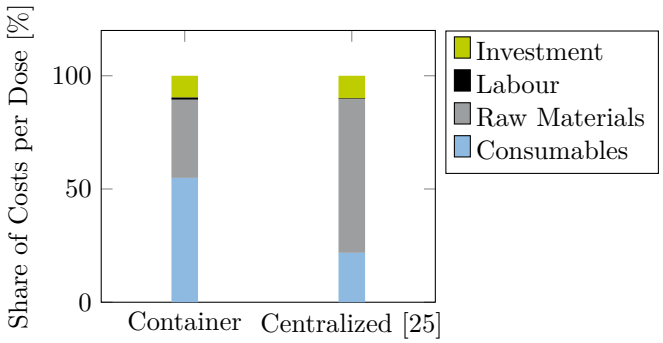

Figure 13: Cost structure of a decentralized container concept (this work) and a centralized facility [25]

5.3. Sensitivity Analysis

The sensitivity analysis aims to identify uncertainties within the proposed concept and the resulting influence on the manufacturing cost. Thus, the influences on the price per dose of different cases are investigated for process parameters, economic parameters and a pharmaceutical aspect. The result of the study is shown in Figure 14. The ordinate shows the different cases that influence the price per dose.

The abscissa shows the percentage influence of the cases on the price of 25.12 €.
The first four categories relate to the influence of the process. The quantity of vaccine doses per batch has a strong effect on the cost per dose, due to the costs of consumables such as filters, tubes, pump heads and most importantly microfluidic cartridges for LNP production remaining almost constant with an increasing batch size. As the concept of economic scale suggests, process scaling should be considered. However, further upscaling not only contradicts the idea of the container as a just-in-time local vaccine production, but is also very much limited at around 10,000 doses, as discussed in section 6.1. Cost fluctuations in the yield of the transcription, represented by the titre of mRNA, are in the single-digit range. The reuse of the affinity chromatography resin would result in a deviation from the single-use concept, but savings of about 10.5% are possible if the resin is used ten times. Similar results can be achieved by using an AEC with a recovery of 86.6% [44].

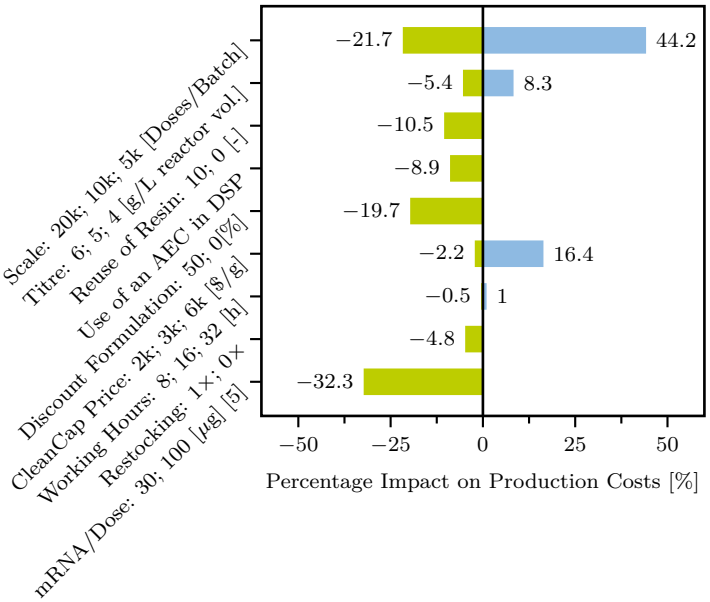

Figure 14: Cost sensitivity regarding assumptions

Considering economic aspects, the GMP system from Precision Nanosystem should be highlighted as a major cost driver. The cost of processing a single batch is estimated by the company to an amount of 100,000 € regardless of the batch size [52]. In the analysis, this cost item was halved, as Precision pointed out that costs for a non-profitable organization or for the purchase of larger quantities would result in price reductions. This assumption reduces the price per dose by 20%. The reagent CleanCap® is the most expensive raw material. For a batch size of 10,000 doses per batch, the influence of the raw materials is not of highest importance. However, further upscaling of the process size will increase the relative influence of this. The influence of labour costs is negligible. Resupplying the container with raw material and reusing the bought equipment will result in spreading the investment costs over more than one million doses which has a minor influence on the price per dose.
Finally, the efficacy of the vaccine is associated with a significant uncertainty. For a conservative estimate of the process, a vaccination dose of 100 μg of mRNA is assumed. This corresponds to the amount of mRNA used in the Moderna vaccine. The product produced by BionTech/Pfizer requires 30 μg per dose. Scaling down the process to produce 10,000 vaccine doses, of 30 μg instead of 100 μg each results in a significant price reduction of the vaccine.
The combination of the shown limits in the analysis allows an estimation for the minimum and maximum price per dose. Thus, a deterioration of the process condition in terms of a lower titre and a smaller batch size in combination with a higher price of the Cap Reagent leads to a price of 44.94 €. Considering the various technical improvements as well as the use of economies of scale in combination with cost reductions for raw and process materials, a significant reduction of the price can be achieved. If combined with the possible improvement in the efficacy of the vaccine, these improvements correspond to a minimum price for the container concept of 3.79 € per dose.

6. Discussion

6.1. Discussion of the Production Scale

As shown in section 5.3, producing large batches comes with a significant economic advantage. In this section, the limits of the batch size and their implications for the overall concept are discussed. While the space time yield of the IVT reaction is not impressive by chemical engineering standards, it is enormous expressed in terms of doses per volume per batch: 5 g or at least 50,000 doses per one liter batch (before downstream processing). When upscaling the batch size within the presented concept, the downstream processing, in particular the second TFF and the AC, will be the first factors to limit a further increase in size. They require 21.2 and 13.7 L of fresh buffer, respectively at the present scale, which is at the limit of what the TFF system can process. This can, at the cost of storage space, be overcome, e.g. by using the next larger TFF system by Repligen, the KMPi, and facilitating fluid handling by the operator through using several bags at a time. Eventually, with further increasing scale, LNP formulation and packaging unit will limit the production capacity, a bottleneck that also holds for very large scale [25]. Note that despite the fluid volumes used in the TFFs limiting the production scale, a substantially larger number of doses per batch is still possible in a scenario, where less than the assumed 100 μg mRNA are needed per dose. For instance, 33,333 doses of 30 μg mRNA [5], can be produced in one batch instead of 10,000 doses of 100 μg. This scenario would require the same amount of raw and single-use (SU) materials, but empty vials would need to be restocked three times.
The production capacity of the container interacts significantly with the intended application and requirements of the local logistics. Not considering resupply of raw materials, it takes the container at least 100 days to run through its stock of raw materials. This corresponds to the duration of a vaccination campaign and can therefore be compared to the duration witness during the COVID-19 pandemic. When vaccinating with the pace witnessed in Israel between 2020/12/19 and 2021/03/16, one of the quickest worldwide, about 130 days are needed to vaccinate 80% of the population [75]. Therefore, the rate at which the containers can process the stored raw materials does not limit the vacci-

nation rate even for 10,000-dose batches.
Accordingly, a useful production scheme would be to produce as large of a batch as possible (10,000 doses for the base case) and stretch the vaccination campaign according to local vaccination centers' capacities by producing only every few days and storing the product in the meantime. This scheme is economically attractive, as savings can be realized by spreading the cost of using the formulation device between more doses (see section 5.3). The area supplied by one container pair in this scenario results from the production capacity over the container's lifetime and the local population density and is discussed in section 6.2.
Comparing the presented concept to a centralized plant, several advantages and drawbacks of the modular and centralized approach come to light. The major advantage of a centralized plant the are lower production costs. As shown in section 5.2, vaccine production can benefit significantly from economics of scale. Another advantage of a centralized over distributed production as presented herein is the capability to achieve a higher vertical integration, allowing the manufacturer to bypass supply bottlenecks. For instance, while RNA vaccine production is ramped up globally, supply bottlenecks can temporally occur in plasmid DNA production [76].
The small modular concept, on the other hand, comes with several less quantifiable, but nonetheless significant advantages. The concept relies on a numbering up [8], rather than a scale-up strategy, which may come with some cost benefits as shortly mentioned in section 5.3.
The eliminated necessity of upscaling comes with the additional advantage of immediate transition from drug development and testing to large-scale production and therefore a faster time to market. Upscaling a production process several times beginning from the small scale used in the early test phases is costly, time-intensive and can result in suboptimal yields [77]. Shifting the production to the site and time of demand helps reduce the additional expenses spent for logistics compared to a large centralized plant.

6.2. Logistics Case Study

Numerous publications have targeted the optimization of vaccine production and distribution via mathematical programming. Those included contributions that focused on the vaccine supply in countries of the global south [78], highlighting current vaccine distribution networks [79–81], the cost of immunization programs [82], social equity of vaccine distribution [83, 84], and energy efficiency [85]. However, all of these works considered solely storage and distribution to take place in middle- and low-income countries, thereby assuming large-scale centralized production of the vaccine presumably in industrialized countries. Therefore, the optimal location of the conceptualized unit is of interest. The 10,000-dose-per-day container as presented herein carries enough raw material to supply 100 batches without resupply. In the following, a strategy is presented on how to rationally distribute such containers in a country or region. In a comparative case-study, an optimization framework is applied using regional population data of two sub-saharan countries, namely Namibia and Nigeria, that both have roughly the same areal size. The two countries were chosen with respect to their respective population density, with Nigeria being rather densely populated at 215 $pop./km^2$ and Namibia being one of the most sparsely populated countries world-wide at 3 $pop./km^2$ [86]. The data for Nigeria included 774 Local Government Areas (LGAs) with their respective population adding up to 193 mio. inhabitants [87, 88], and 121 Constituencies of Namibia, totaling 2.1 mio. inhabitants [89, 90]. The problem was formulated mathematically as a time-invariant capacitated facility location problem (with additional constraints) [91] to obtain optimal locations to deploy the units. Therefore, the total duration of a vaccination campaign is not of interest but only bounded by the maximum of 100 produced batches without resupply. Additional model assumptions included:

- Each unit has a single-use capacity of 1 mio. doses
- A unit consists of 2 containers (section 4.3)
- Vaccination requires 2 doses per patient
- Heard immunity is achieved at a regional vaccination rate of 80%
- Local bottlenecks due to infrastructure, storage and healthcare facilities are neglected

The required number of production facilities forms the objective function which accounts for costs of a vaccination campaign. Thus, it is minimized subject constraints deducted from the assumptions and a constraint on the delivery distance of the produced vaccine. The linear program was implemented using GAMS™ with IBM's ILOG CPLEX™ solver on an Intel64 Family 6 Model with 2.6 GHz and 150 MB RAM. The relative optimality tolerance was 10^{-3} (SI 8).
The optimal spatial distribution of the minimum number of units with a constraint on the delivery distance d_{max} of e.g., 50 km and 500 km respectively is given in figure 15. In the latter case ($d_{max} = 500$ km) the distance delivery constraint is not binding for both respected countries of deployment. In this case, larger capacities of the units or large-scale centralized production would be sensible, as there is no incentive for a small process-scale. In the densely populated case (Nigeria), the container's max. capacity becomes binding around $d_{max} = 80$ km. In case of Namibia however, the container's capacity becomes binding only at $d_{max} = 440$ km. If the viable distribution distances fall short of these characteristic distances, excess capacities of facilities are needed to meet the demand. More generally speaking, constraints imposed by the local vaccine distribution network could lead to a rise in cost per vaccinated person and therefore cost of the whole vaccination campaign.
Apart from these implications for logistics/supply chain, the optimization yields a rough estimation of the number of units for two example countries. However, the smaller d_{max} is chosen, the larger the bias in the solution to be expected, due to the off-grid underlying spatial data. Overall, the optimization results imply an impetus for mobile production units of proposed dimensions of single-use production capacity, especially in sparsely populated regions to counter long and cooling-intensive supply-chains. Nevertheless, local storage hubs and health care facilities ought to be considered for a more rigorous analysis.
Approaches regarding the availability of local storage hubs and health care facilities that enable the last mile distribution of the vaccine ought to be discussed. Time-dependent

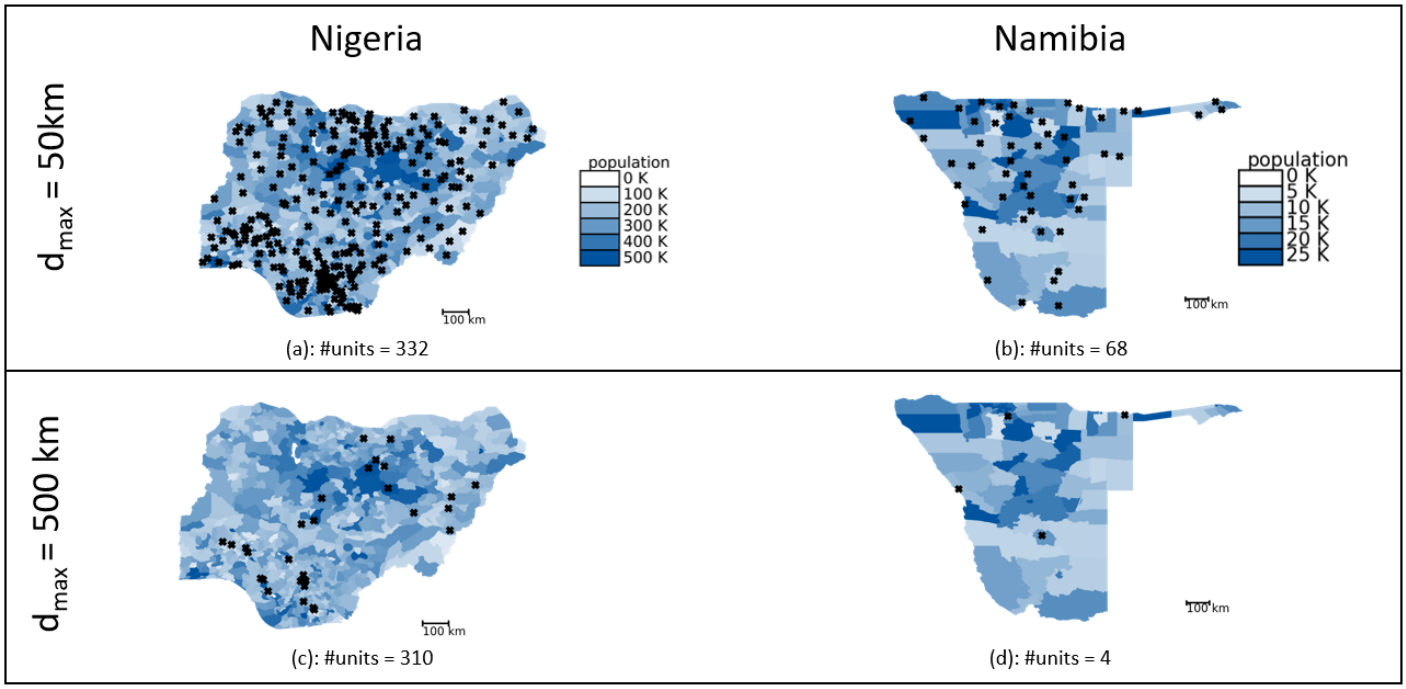

Figure 15: Case study results for Nigeria & Namibia: Number of units under different distance constraints (d_{max})

mathematical programs like e.g. vehicle routing problem on infrastructural data [92, 93] or optimal disease control [94] are promising techniques to further quantify the viability of the proposed mobile on-demand production. More elaborate models of vaccine production and distribution targeting disease dynamics are beyond the scope of this paper.

6.3. Waste Management

For the realisation of the container concept, SU equipment is used in order to avoid contamination of the production process. This approach can be compared with that of stainless steel-based biochemical plant. Case studies in this area indicate that the use of SU materials is less environmentally impactful than traditional biomanufacturing approaches like steam in place [95, 96]. Furthermore, the environmental impacts associated with the disposal of SU components at the end of life are negligible in the context of a life cycle of a biomanufactur [95, 96]. This is of course, if waste is handled properly.

The plastic waste can be further divided into items which have contact to materials like the DNA, mRNA or polymerase and ones which do not. The items which come in contact with these components have to be stored in a double bag at the production site. The packaging plastic waste can be disposed of through the local waste management system. If adequate recycling of the latter cannot be guaranteed locally, all plastic waste produced can be kept inside the container until the raw materials run out (i.e. the vaccination campaign ends), as the used devices and sold vials free up enough space to do so. After the campaign, the containers can be picked up with the waste in them and optionally be restocked and redeployed.

In addition to disposable equipment as a waste category, process streams such as buffer solutions from the TFFs should also be mentioned. About 43 litres of solvent contaminated with DNA, mRNA, lipids or polymerase are produced per batch. Based on the assessment of the Robert Koch Institute, the mRNA vaccines are not considered hazardous to health [97]. In addition to this assessment, it is possible to evaluate the substances with regard to their biosafety level. In the whole process no active viruses or living organisms are used which can cause danger to its surroundings. Thus, no risk in connection with diseases in healthy human adults is expected from the substances used, which corresponds to biosafety level 1. Nevertheless, care should be taken to handle liquid waste responsibly by placing it in a labeled, sealed, leak-proof container. Bleach treatment should be performed after each batch or multiple batch storage to decontaminate the wastewater prior to discharge [98, 99].

7. Conclusion

Container-based on-demand manufacture of mRNA vaccine can be a competitive strategy to combat outbreaks of infectious diseases. While small-scale manufacture is expected to come at an elevated cost as compared to centralized production, the cost of production in a container-based unit (25 €) remains on the order of standard asking prices for vaccines today, even at very conservative assumptions. For more favourable assumptions, in particular with respect to proprietary formulation technology used, the cost of small scale manufacture approaches the cost of centralized production, which is driven by raw material costs. The competitiveness of the manufacturing container dwindles as the batch size is reduced significantly below 10,000 doses or 1 g mRNA per batch. This indicates that for very local outbreaks, e.g. outbreaks associated with refugee camps and natural disasters, the container solution should not be chosen over off-site production and import.

The presented solution allows manufacturing 100 batches, or 1,000,000 vaccine doses remotely with the only resupply required being the one of electricity and drinking water.

This allows supplying remote regions as well as ones barricaded due to local conflicts. The modular nature of the concept allows supplying urban areas by installing multiple containers as well as rural areas. For regions of low population density, the containers' catchment areas can become relatively large and the local infrastructure must be used to distribute the vaccine locally.
The chosen vaccine platform is very versatile and a new mRNA vaccine can be manufactured by using a new DNA template, making virtually no changes to the process itself. When responding to a new pathogen, a single container can be used to conduct tests. By using a number-up rather than scale-up strategy, the production process used in this container can be used as is for large-scale production, potentially leading to an extremely short time to market. Finally, the proposed concept relies exclusively on technology available today and can be operated by relatively low-skilled personnel after basic training.

Supplementary Information is attached

References

1. Eaton, L. Covid-19: WHO warns against "vaccine nationalism" or face further virus mutations. *BMJ (Clinical research ed.)* **372,** n292 (2021).
2. Fontanet, A. *et al.* SARS-CoV-2 variants and ending the COVID-19 pandemic. *The Lancet* **397,** 952–954. ISSN: 01406736 (2021).
3. Wang, Z. *et al.* mRNA vaccine-elicited antibodies to SARS-CoV-2 and circulating variants. *bioRxiv : the preprint server for biology* (2021).
4. Eskier, D., Karakülah, G., Suner, A. & Oktay, Y. RdRp mutations are associated with SARS-CoV-2 genome evolution. *PeerJ* **8,** e9587. ISSN: 2167-8359 (2020).
5. Crommelin, D. J. A., Anchordoquy, T. J., Volkin, D. B., Jiskoot, W. & Mastrobattista, E. Addressing the Cold Reality of mRNA Vaccine Stability. *Journal of pharmaceutical sciences* (2020).
6. Crowell, L. E. *et al.* On-demand manufacturing of clinical-quality biopharmaceuticals. *Nature biotechnology* (2018).
7. Singh, R. *et al.* Systematic substrate adoption methodology (SAM) for future flexible, generic pharmaceutical production processes. *Computers & Chemical Engineering* **58,** 344–368. ISSN: 00981354 (2013).
8. Wohlgemuth, R., Plazl, I., Žnidaršič-Plazl, P., Gernaey, K. V. & Woodley, J. M. Microscale technology and biocatalytic processes: opportunities and challenges for synthesis. *Trends in biotechnology* **33,** 302–314 (2015).
9. Yazdan Panah, B. *et al.* WO2020002598A1. WO2020002598A1 (2020).
10. Plotkin, S., Robinson, J. M., Cunningham, G., Iqbal, R. & Larsen, S. The complexity and cost of vaccine manufacturing - An overview. *Vaccine* **35,** 4064–4071 (2017).
11. Crommelin, D. J. A., Sindelar, R. D. & Meibohm, B. *Pharmaceutical Biotechnology* ISBN: 978-3-030-00709-6 (Springer International Publishing, Cham, 2019).
12. Blakney, A. K., Ip, S. & Geall, A. J. An Update on Self-Amplifying mRNA Vaccine Development. *Vaccines* **9.** ISSN: 2076-393X (2021).
13. Kühnapfel, J. B. *Nutzwertanalysen in Marketing und Vertrieb* ISBN: 978-3-658-25163-5 (Springer Fachmedien Wiesbaden, Wiesbaden, 2019).
14. Zhao, Q. *et al.* In-depth process understanding of RECOMBIVAX HB® maturation and potential epitope improvements with redox treatment: multifaceted biochemical and immunochemical characterization. *Vaccine* **29,** 7936–7941 (2011).
15. Lalonde, M.-E. & Durocher, Y. Therapeutic glycoprotein production in mammalian cells. *Journal of biotechnology* **251,** 128–140 (2017).
16. Kis, Z., Shattock, R., Shah, N. & Kontoravdi, C. Emerging Technologies for Low-Cost, Rapid Vaccine Manufacture. *Biotechnology journal* **14,** e1800376 (2019).
17. Thanh Le, T. *et al.* The COVID-19 vaccine development landscape. *Nature reviews. Drug discovery* **19,** 305–306 (2020).
18. Le, T. T., Cramer, J. P., Chen, R. & Mayhew, S. Evolution of the COVID-19 vaccine development landscape. *Nature reviews. Drug discovery* **19,** 667–668 (2020).
19. Le, T. T., Cramer, J. P., Chen, R. & Mayhew, S. Evolution of the COVID-19 vaccine development landscape. *Nature reviews. Drug discovery* **19,** 667–668 (2020).
20. Cho, H., Excler, J.-L., Kim, J. H. & Yoon, I.-K. Development of Middle East Respiratory Syndrome Coronavirus vaccines - advances and challenges. *Human vaccines & immunotherapeutics* **14,** 304–313 (2018).
21. Watson Marlow. *FPC60: Fill/Finish-System mit einzigartigen Konfigurationsmöglichkeiten* 2021. `https://www.wmftg.com/de-de/range/flexicon/fully-automatic-filling/fpc60-vial-filling-system/` ().
22. generi biotech. *Plasmid linearization* 2021. `https://www.generi-biotech.com/products/plasmid-linearization/` ().
23. generi biotech. *e-Mail conversation with representatives from generi biotech, on 13-18 January 2021*
24. Henderson, J. M. *et al.* Cap 1 Messenger RNA Synthesis with Cotranscriptional CleanCap® Analog by In Vitro Transcription. *Current protocols* **1,** e39 (2021).
25. Kis, Z., Kontoravdi, C., Shattock, R. & Shah, N. Resources, Production Scales and Time Required for Producing RNA Vaccines for the Global Pandemic Demand. *Vaccines* **9.** ISSN: 2076-393X (2020).
26. Hu, C., Cheng, X., Lu, Y., Wu, Z. & Zhang, Q. Gram-scale production of plasmid pUDK-HGF with current good manufacturing practices for gene therapy of critical limb ischemia. *Preparative biochemistry & biotechnology* **46,** 844–849 (2016).
27. Espeseth, A. S. *et al.* Modified mRNA/lipid nanoparticle-based vaccines expressing respiratory syncytial virus F protein variants are immunogenic and protective in rodent models of RSV infection. *NPJ vaccines* **5,** 16 (2020).
28. Hassett, K. J. *et al.* Optimization of Lipid Nanoparticles for Intramuscular Administration of mRNA Vaccines. *Molecular therapy. Nucleic acids* **15,** 1–11. ISSN: 2162-2531 (2019).
29. Rosigkeit, S. *et al.* Monitoring Translation Activity of mRNA-Loaded Nanoparticles in Mice. *Molecular pharmaceutics* **15,** 3909–3919 (2018).
30. Rhoads, R. E. *Synthetic mRNA* ISBN: 978-1-4939-3623-6 (Springer New York, New York, NY, 2016).
31. Jackson, L. A. *et al.* An mRNA Vaccine against SARS-CoV-2 - Preliminary Report. *The New England journal of medicine* (2020).
32. Muttach, F., Muthmann, N. & Rentmeister, A. Synthetic mRNA capping. *Beilstein journal of organic chemistry* **13,** 2819–2832. ISSN: 1860-5397 (2017).
33. Fuchs, A.-L., Neu, A. & Sprangers, R. A general method for rapid and cost-efficient large-scale production of 5' capped RNA. *RNA (New York, N.Y.)* **22,** 1454–1466 (2016).
34. Ramanathan, A., Robb, G. B. & Chan, S.-H. mRNA capping: biological functions and applications. *Nucleic acids research* **44,** 7511–7526 (2016).
35. Kowalski, P. S., Rudra, A., Miao, L. & Anderson, D. G. Delivering the Messenger: Advances in Technologies for Therapeutic mRNA Delivery. *Molecular therapy : the journal of the American Society of Gene Therapy* **27,** 710–728 (2019).
36. Gagnon, P., Persic, S., Goricar, B. & Cernigoj, U. A New Runway for Purification of Messenger RNA. `https://bioprocessintl.com/downstream-processing/separation-purification/a-new-runway-for-mrna-purification/` (2020).
37. Zhong, Z. *et al.* mRNA therapeutics deliver a hopeful message. *Nano Today* **23,** 16–39. ISSN: 17480132 (2018).
38. Easton, L. E., Shibata, Y. & Lukavsky, P. J. Rapid, nondenaturing RNA purification using weak anion-exchange fast performance liquid chromatography. *RNA (New York, N.Y.)* **16,** 647–653 (2010).
39. Karikó, K., Muramatsu, H., Ludwig, J. & Weissman, D. Generating the optimal mRNA for therapy: HPLC purification eliminates immune activation and improves translation of nucleoside-modified, protein-encoding mRNA. *Nucleic acids research* **39,** e142 (2011).
40. Samanta, S. & Martin, C. T. Insights into the mechanism of initial transcription in Escherichia coli RNA polymerase. *The Journal of biological chemistry* **288,** 31993–32003 (2013).
41. Nelson, J. *et al.* Impact of mRNA chemistry and manufacturing process on innate immune activation. *Science advances* **6,** eaaz6893 (2020).
42. Berlanda Scorza, F., Wen, Y.-i., Geall, A. & Porter, F. WO2014140211A1. WO2014140211A1 (2014).
43. Thermo Scientific. *POROS™ Oligo (dT)25 Affinity Resin* 2020. `https://www.thermofisher.com/order/catalog/product/A47382?de&en#/A47382?de&en` ().
44. Issa, William, Joseph, Aunis, John, Grant & Bancel, S. WO2014152031A1. WO2014152031A1 (2014).
45. William Joseph Issa, Joseph Louis Barberio, John Grant Aunins & Noubar B. Afeyan US10590161B2. US10590161B2 (2020).

46. Englezou, P. C. *et al.* Self-Amplifying Replicon RNA Delivery to Dendritic Cells by Cationic Lipids. *Molecular therapy. Nucleic acids* **12,** 118–134. ISSN: 2162-2531 (2018).

47. Guevara, M. L., Persano, F. & Persano, S. Advances in Lipid Nanoparticles for mRNA-Based Cancer Immunotherapy. *Frontiers in chemistry* **8,** 589959. ISSN: 2296-2646 (2020).

48. Wang, J., Peng, Y., Xu, H., Cui, Z. & Williams, R. O. The COVID-19 Vaccine Race: Challenges and Opportunities in Vaccine Formulation. *AAPS PharmSciTech* **21,** 225 (2020).

49. ModernaTX, C. https://www.modernatx.com/sites/default/files/mRNA-1273-P301-Protocol.pdf ().

50. Precision Nanosystems. *mRNA Lipid Nanoparticles Robust low-volume production for screening high-value nanoparticle materials* 2021. Article,%20Brochure ().

51. Richner, J. M. *et al.* Modified mRNA Vaccines Protect against Zika Virus Infection. *Cell* **168,** 1114–1125.e10 (2017).

52. Precision Nanosystems. *Video conversation with representatives from Precision Nanosystems, 24 February 20201*

53. Reichmuth, A. M., Oberli, M. A., Jaklenec, A., Langer, R. & Blankschtein, D. mRNA vaccine delivery using lipid nanoparticles. *Therapeutic delivery* **7,** 319–334 (2016).

54. Bancel, S., William, J., John, Aunins, John Grant & Charkraborty, T. WO2014152027A1. WO2014152027A1

55. Kranz, L. M. *et al.* Systemic RNA delivery to dendritic cells exploits antiviral defence for cancer immunotherapy. *Nature* **534,** 396–401 (2016).

56. European Medicines Agency. Guideline on the quality, non-clinical and clinical aspects of gene therapy medicinal products (2018).

57. FDA/CBER. Development and Licensure of Vaccines to Prevent COVID-19: Guidance for Industry (2020).

58. Poveda, C., Biter, A. B., Bottazzi, M. E. & Strych, U. Establishing Preferred Product Characterization for the Evaluation of RNA Vaccine Antigens. *Vaccines* **7.** ISSN: 2076-393X (2019).

59. Bahl, K. *et al.* Preclinical and Clinical Demonstration of Immunogenicity by mRNA Vaccines against H10N8 and H7N9 Influenza Viruses. *Molecular therapy : the journal of the American Society of Gene Therapy* **25,** 1316–1327 (2017).

60. Schmid, A. Considerations for Producing mRNA Vaccines for Clinical Trials. *Methods in molecular biology (Clifton, N.J.)* **1499,** 237–251 (2017).

61. Intelligen. *SuperPro Designer* 2000. https://www.intelligen.com/products/superpro-overview/.

62. Merckmillipore. *Mobius 3L Single-use Bioreactor* 2020. https://www.merckmillipore.com/DE/de/product/Mobius-3L-Single-use-Bioreactor,MM_NF-C84539?.

63. Repligen. *KrosFlo® KR2i Tangential Flow Filtration (TFF) System* 2020. https://www.repligen.com/technologies/krosflo-tff/lab/kr2i ().

64. precision nanosystems. *NanoAssemblr GMP system* 2020. https://www.precisionnanosystems.com/platform-technologies/product-comparison/gmp-system ().

65. Stéphane Mabic, I. K. *Production of ultrapure water for RNase-sensitive applications via ultrafiltration* 2012.

66. Green, M. R. & Sambrook, J. How to Win the Battle with RNase. *Cold Spring Harbor protocols* **2019** (2019).

67. Filina-Dawidowicz, L. & Filin, S. Innovative energy-saving technology in refrigerated containers transportation. *Energy Efficiency* **12,** 1151–1165. ISSN: 1570-646X (2019).

68. Złoczowska, E. Maritime Containers Refrigeration Plant Faults Survey. *New Trends in Production Engineering* **1,** 589–595 (2018).

69. World Health Organization. *Supplementary guidelines on good manufacturing practices for heating, ventilation and airconditioning systems for non-sterile pharmaceutical dosage forms* 2011.

70. cleanroomworld. *HEPA Filtered AC Unit, 2 tons* 2020. https://cleanroomworld.com/cleanroom-equipment/hepa-ac-units/cleanroom-ac-filters-2-ton/ ().

71. Payne, V. & Domanski, P. A Comparison Of An R22 And An R410A Air Conditioner Operating At High Ambient Temperatures. *International Refrigeration and Air Conditioning Conference* (2002).

72. Tesla. *Tesla PowerWall* 2020. https://www.tesla.com//powerwall ().

73. Tagesschau; Source: Norddeutscher Rundfunk, Westdeutscher Rundfunk Koeln and Sueddeutsche Zeitung. *Offenbar deutlich niedrigeren Preis durchgesetzt* 2021. https://www.tagesschau.de/investigativ/ndr-wdr/corona-impfstoff-biontech-105.html ().

74. Kis, Z. *e-Mail conversation with Zoltan Kis; on 31 March 2021*

75. Israel Ministry of Health. *Corona virus in Israel - general situation* 2021. https://datadashboard.health.gov.il/COVID-19/general ().

76. Ohlson, J. Plasmid manufacture is the bottleneck of the genetic medicine revolution. *Drug discovery today* (2020).

77. Lewin, J. J., Choi, E. J. & Ling, G. Pharmacy on demand: New technologies to enable miniaturized and mobile drug manufacturing. *American journal of health-system pharmacy : AJHP : official journal of the American Society of Health-System Pharmacists* **73,** 45–54 (2016).

78. Boeck, K. D., Decouttere, C. & Vandaele, N. *Vaccine distribution supply chains in developing countries: A literature review* Working Papers of Department of Decision Sciences and Information Management, Leuven 629348 (KU Leuven, Faculty of Economics, Business (FEB), Department of Decision Sciences, and Information Management, Leuven, Nov. 2018). https://ideas.repec.org/p/ete/kbiper/629348.html.

79. Chen, S.-I. *et al.* A planning model for the WHO-EPI vaccine distribution network in developing countries. *IIE Transactions* **46,** 853–865. ISSN: 0740-817X (2014).

80. Hirsh Bar Gai, D., Graybill, Z., Voevodsky, P. & Shittu, E. Evaluating scenarios of locations and capacities for vaccine storage in Nigeria. *Vaccine* **36,** 3505–3512 (2018).

81. Yang, Y., Bidkhori, H. & Rajgopal, J. Optimizing vaccine distribution networks in low and middle-income countries. *Omega* **99,** 102197. ISSN: 03050483 (2021).

82. Bulula, N., Mwiru, D. P., Swalehe, O. & Thomas Mori, A. Vaccine storage and distribution between expanded program on immunization and medical store department in Tanzania: a cost-minimization analysis. *Vaccine* **38,** 8130–8135 (2020).

83. Rastegar, M., Tavana, M., Meraj, A. & Mina, H. An inventory-location optimization model for equitable influenza vaccine distribution in developing countries during the COVID-19 pandemic. *Vaccine* **39,** 495–504 (2021).

84. Enayati, S. & Özaltın, O. Y. Optimal influenza vaccine distribution with equity. *European Journal of Operational Research* **283,** 714–725. ISSN: 03772217 (2020).

85. Lloyd, J., McCarney, S., Ouhichi, R., Lydon, P. & Zaffran, M. Optimizing energy for a 'green' vaccine supply chain. *Vaccine* **33,** 908–913 (2015).

86. IDA, T. W. B. I. 2021. https://data.worldbank.org/indicator/EN.POP.DNST?name_desc=true ().

87. National Population Commission of Nigeria, N. B. o. S. https://www.citypopulation.de/php/nigeria-admin.php ().

88. Office for the Surveyor General of the Federation of Nigeria E Health, U. N. C. S. U. https://data.humdata.org/dataset/nga-administrative-boundaries ().

89. Agency, N. S. https://www.citypopulation.de/en/namibia/admin/ ().

90. Tatem, A. https://energydata.info/dataset/namibia-population-density-2015 ().

91. Melkote, S. & Daskin, M. S. Capacitated facility location/network design problems. *European journal of operational research* **129,** 481–495 (2001).

92. Al Theeb, N., Smadi, H. J., Al-Hawari, T. H. & Aljarrah, M. H. Optimization of vehicle routing with inventory allocation problems in Cold Supply Chain Logistics. *Computers & Industrial Engineering* **142,** 106341. ISSN: 03608352 (2020).

93. Miller, C. E., Tucker, A. W. & Zemlin, R. A. Integer Programming Formulation of Traveling Salesman Problems. *Journal of the ACM* **7,** 326–329. ISSN: 0004-5411 (1960).

94. Hezam, I. M., Foul, A. & Alrasheedi, A. A dynamic optimal control model for COVID-19 and cholera co-infection in Yemen. *Advances in Difference Equations* **2021,** 108. ISSN: 1687-1847. https://doi.org/10.1186/s13662-021-03271-6 (2021).

95. Shukla, A. A. & Gottschalk, U. Single-use disposable technologies for biopharmaceutical manufacturing. eng. *Trends in biotechnology* **31.** Journal Article Review, 147–154. eprint: 23178074 (2013).

96. Whitford, W. G., Petrich, M. A. & Flanagan, W. P. in *SingleâUse Technology in Biopharmaceutical Manufacture* 169–179 (John Wiley & Sons, Ltd, 2019). ISBN: 9781119477891.

97. Umweltbundesamt. *Hinweise zur Entsorgung von Abfaellen aus Massnahmen zur Eindaemmung von COVID 19* 2021. https://www.umweltbundesamt.de/sites/default/files/medien/421/dokumente/hinweise_zur_entsorgung_von_abfaellen_aus_massnahmen_zur_eindaemmung_von_covid_stand_16.3.21.pdf ().

98. University of Glasgow. *CLASSIFYING BIOLOGICAL HAZARDS* 2021. https://www.gla.ac.uk/myglasgow/seps/az/biological%5C%20safety/transport%5C%20of%5C%20biological%5C%20hazards/classifying%5C%20biological%5C%20hazards/ ().

99. Environmental Health and Safety University of Washington. *Biohazardous Waste Streams* 2021. https://www.ehs.washington.edu/system/files/resources/lsb-waste.pdf ().